

Title: Practical Clinical Measurement of Radiotracer Concentration in Blood – Initial Device Concept and Feasibility Testing

Josh Knowland¹, Ronald Lattanze¹, Jesse Kingg¹, Steven Perrin¹

¹Lucerno Dynamics, Cary, NC

Corresponding Author:

Josh Knowland

Lucerno Dynamics

140 Towerview Court

Cary, NC 27513

919-371-6800

jknowland@lucernodynamics.com

word count: 2,671

Short Running Title: Measurement of Radiotracer in Blood

Immediate Open Access: Creative Commons Attribution 4.0 International License (CC BY) allows users to share and adapt with attribution, excluding materials credited to previous publications.

License: <https://creativecommons.org/licenses/by/4.0/>.

Details: <http://jnm.snmjournals.org/site/misc/permission.xhtml>.

Abstract

Kinetic analysis of PET data requires continuous measurement of radioactivity in the arterial blood throughout the acquisition time, termed the arterial input function (AIF). The AIF is used as an input to compartmental modeling, which can be a better predictor of disease progression than SUV measurements from static PET images. Current common methods of measuring blood concentrations include image-derived, population-based, and manual sampling. These all have challenges due to logistical and technological issues as well as patient burden. The aim of this study was to design, develop, and assess a device that is practical and effective for the routine measurement of β -emitting radiotracer concentration in blood without the drawbacks of current methods and where metabolite analysis is not required.

Methods

Designs that integrated a scintillating fiber and a silicon photomultiplier (SiPM) with a general purpose venous access catheter for in vivo measurement were considered. Other design requirements included miniaturization, high sampling rates, and stopping power for β -particles. Preliminary prototypes were designed to test the feasibility of the concept. Phantom tests were developed to mimic human vasculature. Tests of linearity, sensitivity, signal-to-noise ratios (SNR), the impact of vein diameter, and the influence of gamma radiation were conducted.

Results

Prototype sensors were constructed using two different diameters of polystyrene-based scintillating fibers. Fibers were custom polished and fixed to a SiPM. Sensor output was linear with $R^2 = 0.999$ over the range from 0.037 megabecquerels (MBq) per milliliter (mL) to 9.25 MBq/mL. Absolute sensitivity was approximately 450 counts per second (cps) per MBq/mL. Measured SNRs ranged from 1.2:1 to 3.2:1 using a blood to tissue concentration ratio of 1:1. Sensor output increased with vein diameter, and showed no sensitivity to gamma radiation.

Conclusions

In experiments with phantom models, the prototype provided accurate measurements of beta-emitting radiotracer concentration. The design will be refined for in vivo testing. The ability to routinely gather blood input function data would facilitate the adoption of kinetic modeling of PET data.

Key words: AIF, PET, radiotracer, input function

Introduction

The arterial input function (AIF) is used as an input to kinetic analysis, which can be a better predictor of disease progression than SUV measurements from static PET images(1-4). Such analysis requires a continuous measurement of radioactivity in the arterial blood throughout the acquisition time(5).

Current methods for obtaining radiotracer concentration in blood are: population-based input functions (PBIF), image-derived input functions (IDIF), and ex vivo measurement. PBIF data are pre-generated by combining measurements from arterial samples of multiple subjects in a population. IDIF data are individually generated by using volumetric time-slice data from dynamic PET scans in a target area (e.g. wrist artery, internal carotid artery, left ventricle, abdominal aorta). Ex vivo measurements include manual and automated sampling of arterial or arterialized venous blood. The process of arterIALIZING venous blood involves heating of the area of interest. The resulting vasodilation causes localized venous blood to approximate arterial blood. Several authors report that this process is suitable in gathering blood input function data for certain procedures, including FDG studies as glucose does readily shunt from arterial to venous(6-12). Some analyses use drawn blood for metabolite analysis, though in many cases, such as FDG studies, this analysis is not required, though(13).

Manual ex vivo measurement has several challenges. Highly trained staff are required to collect samples and perform measurements in real time during the procedure(14-16). In the process, they are at an increased risk for exposure to radiation and blood pathogens(15,16). Sample rates are limited due to the operations involved, which can lead to under-sampling of the input function(14-16). Human and equipment errors can lead to measurement variability(14-16).

Automatic ex vivo measurements suffer from dispersion effects that must be corrected(14,15). They can require significant shielding(14,15), and multiple system components(16) (e.g., tubing, collection and waste containers, sources of pressure and vacuum), all of which add to complexity.

Both automated and manual blood sampling require equipment sterilization, can cause patient discomfort, can require large volumes of blood to be drawn, and in rare cases, can lead to medical complications(15).

PBIFs also have several challenges. Their creation still requires arterial blood sampling, error-free injections, populations that match the patient (e.g., diabetic, child, obese), and are radiotracer-specific. Use of PBIF for an individual patient also requires a blood sample for scaling(17).

Similarly, IDIFs have drawbacks. They require a large blood pool and the area of interest to be in the same PET imaging bed(18,19). Additionally, they suffer from partial volume effects(19), and are prone to errors due to patient movement and volume of interest definition variability(18).

In addition to the methods referenced above, there are published examples of using small-diameter scintillating plastic fibers to measure radiotracer concentration directly in tissue or blood vessels(20-23). These fibers do not have the stopping power to measure gamma radiation. Instead, they detect β -particles before annihilation and subsequent production of gamma rays used for imaging. The limited range of β -radiation naturally reduces the radius of detection, which is advantageous in that it limits the impact of background radiation from outside of the vessel. Although used for preclinical research, these fiber-based devices are not known to be available for human use. In addition, they suffer from their own limitations including requiring multiple points of vascular access and partial volume effects.

The specific objectives of this study were to design, prototype, and assess a device that is practical and easy-to-use for measuring the concentration of beta-emitting radiotracer in blood. The device addresses many of the drawbacks which limit the adoption of current methods. For cases in which metabolite analysis is required, the device might also be used to draw blood samples.

Materials and Methods

Design Concept

The proposed design consists of a polystyrene-based scintillating fiber that is readily commercially available, has low light loss, is flexible, and has adequate stopping power for β -particles. The fiber is integrated with a general purpose venous access catheter (figure 1). Additionally, a miniature SiPM is contained in the catheter assembly to minimize loss of scintillation light. This design allows measurement of radiotracer concentration in blood without requiring additional venous access. Additional circuitry is contained in a bed-side or wearable data logger, which enables high frame-rate sensor data acquisition.

Prototype Device Construction

For initial evaluation of the proposed design, two prototypes of the scintillating fiber assembly were constructed using fibers of diameter 0.25 mm and 0.5 mm (figure 2). Both fibers were BCF-12 material (Saint-Gobain Crystals, Newbury OH) with emission peak wavelength of 435 nm, 3.2 ns decay time, and $\sim 8,000$ photons/MeV. Each fiber was polished using a custom fixture based on commercially available fiber optic polishing systems. Each fiber was affixed with epoxy (Double/Bubble® #04004, Royal Adhesives & Sealants, LLC, Wilmington, CA) to a polished 3 mm diameter acrylic light guide and custom mounting screw.

The detector was designed to ensure co-planar alignment of the light guide and a 3 mm x 3 mm SiPM (MicroFC-30035-SMT, SensL Technologies, Ltd., Cork Ireland). This SiPM is a good candidate for the design due to its high microcell density, low breakdown voltage, and sensitivity to wavelengths of light produced by the chosen fiber. Optical coupling gel (SS-998, Silicone Solutions, Cuyahoga Falls, OH) enhanced transmission between the light guide and SiPM.

Sensor electronics were based on a transimpedance amplifier front end for read-out of the SiPM. Amplified signals were then screened using a lower level discriminator threshold circuit. Full energy windowing was not used for

thresholding in order to simplify the design. Additionally, by employing a simple asynchronous pulse-counting scheme, sensors obtained a high rate of data acquisition. Sensor hardware counts pulses 99.95% of the time. The remaining time is spent storing and transmitting counts to a connected personal computer. The sensor is susceptible to pulse pile-up dead time, but this phenomenon is lessened by the fast decay time of the plastic scintillation fiber (3.2 ns), high-speed electronics (236 MHz amplifier) and the relatively low count rates expected. Linearity and sensitivity were measured over the range of activities expected, but not to the point where pile-up is evident. Before testing, the lower level discriminator was set just above the level of background electrical noise.

Phantom Testing

All testing was performed within a light-proof box to block ambient light. The experimental setup was positioned behind lead bricks to minimize radiation exposure to personnel.

To simulate human vasculature, artificial veins were made of plastic tubing (0.25 mm to 0.35 mm wall thickness) with internal diameters 2.3 mm, 4.75 mm and 6.3 mm. These diameters represented arm veins commonly used for radiotracer injections in PET procedures(24). One end of each vein was sealed with epoxy. Additionally, a plastic cylinder of 27 mm internal diameter simulated tissue surrounding the artificial veins.

The impact of vein diameter on sensor output was assessed by immersing each fiber in the 2.3 mm and 6.3 mm artificial veins, as well as in the 27 mm cylinder. Each was filled with ^{18}F -FDG of concentration 0.37 MBq/mL.

During a typical injection the radiotracer concentration in blood is expected to vary greatly. Assuming an injected dose of 370 MBq of FDG in a patient of 68 kg, blood concentration within the first 90 seconds is estimated to be 100 kBq/mL. By the two-minute mark, the concentration would drop to approximately 40 kBq/mL, and thereafter slowly drop to approximately 5.5 kBq/mL over the course of an hour(18). Over the same time, the concentration in tissue surrounding the vein would rise to the same approximately 5.5 kBq/mL. Depending on the range of the β -particles, the fiber may detect activity from outside of the vein. This study defined the signal-to-noise ratio as the ratio of measured activity from inside the vein (signal) to that from outside the vein (noise). As the blood to tissue

concentration ratio approaches 1:1 activity from outside of the vein contributes a larger fraction of the particles which are detected. To measure activity from outside the vein, each fiber was inserted into each artificial vein filled with plain water. Measurements were then taken with the water-filled veins inserted into the 27 mm diameter cylinder filled with a 0.37 MBq/mL 18F-FDG solution. Data from the vein diameter impact test were used for the signal portion of the SNR calculation.

Performance Testing

Detector linearity and absolute sensitivity were assessed by taking measurements with the 0.5 mm diameter fiber in a solution of 18F-FDG as it decayed from 9.25 MBq/mL to 0.037 MBq/mL. Temperature compensation of sensor data was performed post-hoc using a linear correction.

Measurement of Gamma vs Beta Emissions

While the travel distance of beta radiation is low, gamma radiation travels much farther and may influence measurements. To measure the detector's sensitivity to gamma radiation, a solution of Tc-99m was prepared with an activity of 19 MBq and placed in a test tube. Tc-99m was chosen for this test for two reasons. First, its 140 keV photons would be more easily stopped by the scintillating fiber than the 511 keV photons of F-18 resulting in higher sensitivity. Secondly, Tc-99m being a pure gamma emitter, removes the possible influence of beta particles on the measurement. The 0.5 mm diameter fiber was first placed 50 mm away from the test tube radially, then 2 mm axially above the test tube, and finally submerged approximately 25 mm into the solution. Measurements were taken at each location.

Results

Linearity

Linearity was calculated by comparing the measured signal to the theoretical level as the isotope decayed over the concentration range of 9.25 MBq/mL to 0.037 MBq/mL. Over this range of concentrations, the system has

sufficient bandwidth that pulse pile-up is not a factor in linearity. See figure 3 for details. Sensor output is linear with $R^2 = 0.999$.

Absolute Sensitivity

Using data measured while the isotope decayed from a concentration of 9.25 MBq/mL to 0.037 MBq/mL, absolute sensitivity was calculated to be approximately 450 cps/MBq/mL. See figure 3 for details. This study did not investigate the relationship between fiber diameter and sensitivity, but smaller diameter fibers would be expected to be less sensitive.

Signal-to-Noise Ratio

See figure 4 for measurements of noise originating from activity outside the vein. Note that this measurement may have been impacted by a lack of centeredness of the fiber within the artificial vein. Results of the signal-to-noise ratio experiment ranged from 1.2:1 to 3.2:1. The scenario tested in this study was worst-case in that the blood to tissue concentration was 1:1, which may occur at the end of uptake. During the majority of the uptake period, the blood to tissue concentration ratio is much higher than 1:1, for instance 25:1, and the SNR improves accordingly.

Impact of Vein Diameter

As vein diameter increases, sensor output should also increase until the radius equals the positron's maximum range (2.16 mm for F-18 in water⁽²⁵⁾). Experimentally, sensor output did increase with vein diameter, but the number of vein diameters tested was insufficient to fully characterize the relationship. See figure 5.

Gamma vs Beta Emissions

The gamma vs beta emission experiments show no response to Tc-99m. All three experimental locations registered zero cps.

Discussion

Kinetic modeling has been shown to be a better predictor of disease progression than static measures in some cases(1-4). Kotasidis, et. al. and Takesh summarize the use of kinetic modeling with various tracers and various pathological conditions with promising results. However, kinetic modeling is difficult to implement in routine clinical practice.(4,13,26). Dunnwald et. al. suggested that the results of their study of kinetic modeling versus static measures in neoadjuvant breast cancer patients should provide an impetus for development of clinically practical approaches for obtaining FDG kinetic measures for tumor response evaluation(2). In order to move kinetic modeling from the realm of drug development and clinical research into everyday clinical use for the benefit of all patients, new ideas must be considered.

An in situ detector design could be a clinically practical approach for measurement of the blood input function without the limitations of current methods. The proposed design may not require arterial blood sampling, complex equipment or shielding, or additional time or exposure risk for staff. Additionally, it would provide a high rate of sensor data acquisition to accurately measure the dynamic concentration fluctuations encountered during and following injection.

However, the full benefits of the proposed design depend on the applicability of venous blood as a surrogate for arterial blood in creation of the input function. Venous, or arterialized venous blood would be advantageous for use with the proposed design because patient discomfort would be limited to one venous access. However, arterIALIZATION of arm or hand blood is not without drawbacks. It typically involves the use of a heating pad or box for several minutes. Additionally, while several authors report that arterIALIZED blood is applicable for glucose measurements(6-12), it is not appropriate for all analyses(27). However, even if this dependency does not apply, the proposed design could still be useful. The design, whether employed as an arterial or venous catheter, could both measure input function data and allow blood sampling for metabolite analysis, etc.

There were limitations to this study. The fiber was not well centered within the artificial veins. This introduced effects where activity outside of the vein was measured unintentionally. The difficulty in centering the fibers during experimental testing was unanticipated, but could be corrected in future designs. Additionally, the limited number of artificial veins tested limited our ability to measure the true fiber detection radius. The inflection point indicating the maximum radius of detection was not evident due to the limited number of diameters tested. While not an issue during this study or with the use of FDG in the clinic, a limitation of the overall concept is that an in situ device without blood sampling could not discriminate between administered radiopharmaceutical and its metabolites(16,28). This study did not test experimentally the lowest activity anticipated after an hour of uptake time of approximately 5.5 kBq/mL. Given the detector's sensitivity of 450 cps/MBq/mL, only 2 cps would be expected at this activity level. In order to adequately measure blood activity for an entire uptake period, detector sensitivity must be improved. However, for FDG, low levels of blood activity are only anticipated during the later part of the uptake period. Blood concentration curves are typically steady during this time and could be extrapolated from the earlier portion of the uptake time.

Further research is required to integrate the fiber with a catheter, develop a mechanism to center the fiber within the vein, investigate methods to control the fiber detection radius, and determine optimal fiber length. Methods for catheter integration and centering the fiber can be informed by existing cardiovascular intravenous catheter technology. In addition, it may be advantageous to include a layer of β -particle shielding between the fiber and the catheter lumen. This could reduce the impact of any radiotracer that remains in the lumen after injection and flush(29). Two possible methods to control the fiber detection radius include adjustment of the lower-level discriminator to discard lower energy particles and application of a thin shielding material over the fiber. These methods would discard or block lower energy particles that tend to have originated farther away. The shielding layer would also provide the benefit of blocking ambient light. Sensitivity of the device is expected to increase with fiber length. However, any scintillating fiber outside of the vein would contribute background noise. A scintillating tip connected to a non-scintillating optical fiber for transmission is one option to alleviate this noise(20,30). However, the two-material approach could cause loss of scintillation light at the junction while also increasing complexity and cost. Studies would be required to determine the optimal fiber configuration.

While additional work is needed, this study demonstrated the feasibility of a detector based on an SiPM and plastic scintillation fiber. As development progresses, validation (e.g., additional bench testing, animal studies, human clinical studies) must be performed against the current methods of AIF measurement.

Conclusion

This study performed initial feasibility testing of a low-cost, disposable, scintillating venous access catheter design that has the potential to provide radiotracer blood concentration data for kinetic modeling. The ability to routinely gather blood input function data would facilitate the adoption of kinetic analysis in the clinic.

References

1. Dimitrakopoulou-Strauss A, Hoffmann M, Bergner R, Uppenkamp M, Haberkorn U, Strauss LG. Prediction of progression-free survival in patients with multiple myeloma following anthracycline-based chemotherapy based on dynamic FDG-PET. *Clin Nucl Med*. 2009;34:576-584.
2. Dunnwald LK, Doot RK, Specht JM, et al. PET tumor metabolism in locally advanced breast cancer patients undergoing neoadjuvant chemotherapy: value of static versus kinetic measures of fluorodeoxyglucose uptake. *Clin Cancer Res*. 2011;17:2400-2409.
3. Nishiyama Y, Yamamoto Y, Monden T, et al. Diagnostic value of kinetic analysis using dynamic FDG PET in immunocompetent patients with primary CNS lymphoma. *Eur J Nucl Med Mol Imaging*. 2007;34:78-86.
4. Takesh M. The Potential Benefit by Application of Kinetic Analysis of PET in the Clinical Oncology. *ISRN Oncol*. 2012;2012:349351.
5. Schaefferkoetter JD, Osman M, Townsend DW. The importance of quality control for clinical PET imaging. *J Nucl Med Technol*. 2017;45:265-266.
6. Brooks DC, Black PR, Arcangeli MA, Aoki TT, Wilmore DW. The heated dorsal hand vein: an alternative arterial sampling site. *JPEN J Parenter Enteral Nutr*. 1989;13:102-105.
7. Copeland KC, Kenney FA, Nair KS. Heated dorsal hand vein sampling for metabolic studies: a reappraisal. *Am J Physiol*. 1992;263:E1010-1014.
8. Huang SC, Phelps ME, Hoffman EJ, Sideris K, Selin CJ, Kuhl DE. Noninvasive determination of local cerebral metabolic rate of glucose in man. *Am J Physiol*. 1980;238:E69-82.
9. Jensen MD, Heiling VJ. Heated hand vein blood is satisfactory for measurements during free fatty acid kinetic studies. *Metabolism*. 1991;40:406-409.
10. Liu D, Moberg E, Kollind M, Lins PE, Adamson U, Macdonald IA. Arterial, arterialized venous, venous and capillary blood glucose measurements in normal man during hyperinsulinaemic euglycaemia and hypoglycaemia. *Diabetologia*. 1992;35:287-290.
11. Phelps ME, Huang SC, Hoffman EJ, Selin C, Sokoloff L, Kuhl DE. Tomographic measurement of local cerebral glucose metabolic rate in humans with (F-18)2-fluoro-2-deoxy-D-glucose: validation of method. *Ann Neurol*. 1979;6:371-388.

- 12.** van der Weerd AP, Klein LJ, Visser CA, Visser FC, Lammertsma AA. Use of arterialised venous instead of arterial blood for measurement of myocardial glucose metabolism during euglycaemic-hyperinsulinaemic clamping. *Eur J Nucl Med Mol Imaging*. 2002;29:663-669.
- 13.** Kotasidis FA, Tsoumpas C, Rahmim A. Advanced kinetic modelling strategies: towards adoption in clinical PET imaging. *Clinical and Translational Imaging*. 2014;2:219-237.
- 14.** Boellaard R, van Lingen A, van Balen SCM, Hoving BG, Lammertsma AA. Characteristics of a new fully programmable blood sampling device for monitoring blood radioactivity during PET. *Eur J Nucl Med*. 2000;28:81-89.
- 15.** Espagnet R, Frezza A, Martin JP, et al. A CZT-based blood counter for quantitative molecular imaging. *EJNMMI Physics*. 2017;4:18.
- 16.** Graham MM, Lewellen BL. High-speed automated discrete blood sampling for positron emission tomography. *J Nucl Med*. 1993;34:1357-1360.
- 17.** Takikawa S, Dhawan V, Spetsieris P, et al. Noninvasive quantitative fluorodeoxyglucose PET studies with an estimated input function derived from a population-based arterial blood curve. *Radiology*. 1993;188:131-136.
- 18.** de Geus-Oei LF, Visser EP, Krabbe PF, et al. Comparison of image-derived and arterial input functions for estimating the rate of glucose metabolism in therapy-monitoring 18F-FDG PET studies. *J Nucl Med*. 2006;47:945-949.
- 19.** Zanotti-Fregonara P, Chen K, Liow JS, Fujita M, Innis RB. Image-derived input function for brain PET studies: many challenges and few opportunities. *J Cereb Blood Flow Metab*. 2011;31:1986-1998.
- 20.** Lee K, Fox PT, Lancaster JL, Jerabek PA. A positron-probe system for arterial input function quantification for positron emission tomography in humans. *Rev Sci Instrum*. 2008;79:064301.
- 21.** Pain F, Laniece P, Mastrippolito R, et al. SIC, an intracerebral radiosensitive probe for in vivo neuropharmacology investigations in small laboratory animals: theoretical considerations and practical characteristics. *IEEE Trans Nucl Sci*. 2000;47:25-32.
- 22.** Pain F, Laniece P, Mastrippolito R, Gervais P, Hantraye P, Besret L. Arterial input function measurement without blood sampling using a beta-microprobe in rats. *J Nucl Med*. 2004;45:1577-1582.
- 23.** Woody CL, Stoll SP, Schlyer DJ, et al. A study of scintillation beta microprobes. *IEEE Trans Nucl Sci*. 2002;49:2208-2212.

24. Spivack DE, Kelly P, Gaughan JP, van Bemmelen PS. Mapping of superficial extremity veins: normal diameters and trends in a vascular patient-population. *Ultrasound Med Biol.* 2012;38:190-194.
25. Cal-Gonzalez J, Herraiz JL, Espana S, et al. Positron range estimations with PeneloPET. *Phys Med Biol.* 2013;58:5127-5152.
26. Muzi M, O'Sullivan F, Mankoff DA, et al. Quantitative assessment of dynamic PET imaging data in cancer imaging. *Magn Reson Imaging.* 2012;30:1203-1215.
27. Green JH, Ellis FR, Shallcross TM, Bramley PN. Invalidity of hand heating as a method to arterialize venous blood. *Clin Chem.* 1990;36:719-722.
28. Warnock G, Bahri MA, Goblet D, et al. Use of a beta microprobe system to measure arterial input function in PET via an arteriovenous shunt in rats. *EJNMMI Research.* 2011;1:13.
29. Ponto LL, Graham MM, Richmond JC, et al. Contamination levels in blood samples drawn from the injection intravenous line. *Mol Imaging Biol.* 2002;4:410-414.
30. Apollinari G, Scepanovic D, White S. Plastic optical fiber splicing by thermal fusion. *Nuclear Instruments and Methods in Physics Research Section A: Accelerators, Spectrometers, Detectors and Associated Equipment.* 1992;311:520-528.

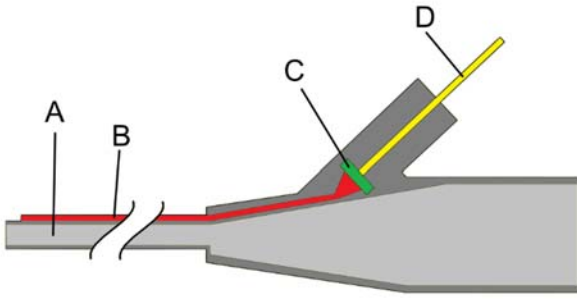


FIGURE 1. Cross-section diagram of proposed scintillation catheter consisting of IV catheter (A), scintillation fiber (B), SiPM (C), and electrical signal wires (D).

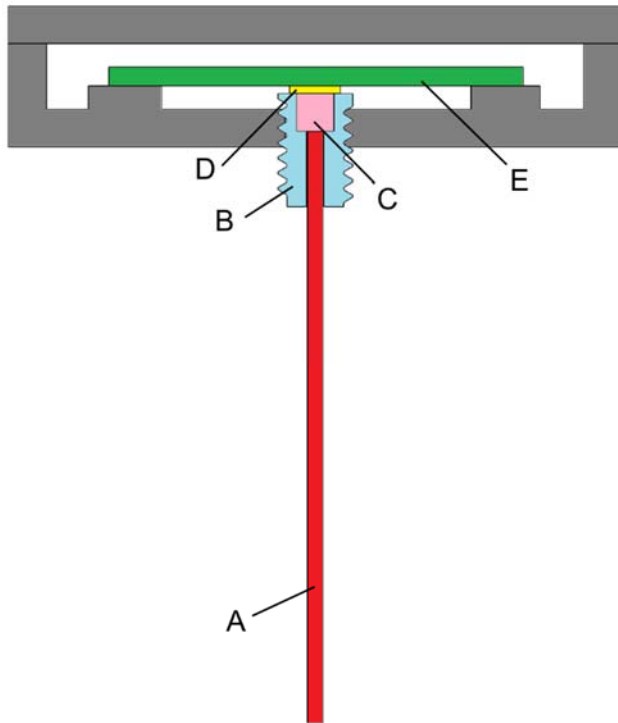


FIGURE 2. Cross-section diagram of prototype detector consisting of scintillation fiber (A), mounting screw (B), acrylic light guide (C), SiPM (D), and electronic circuitry (E).

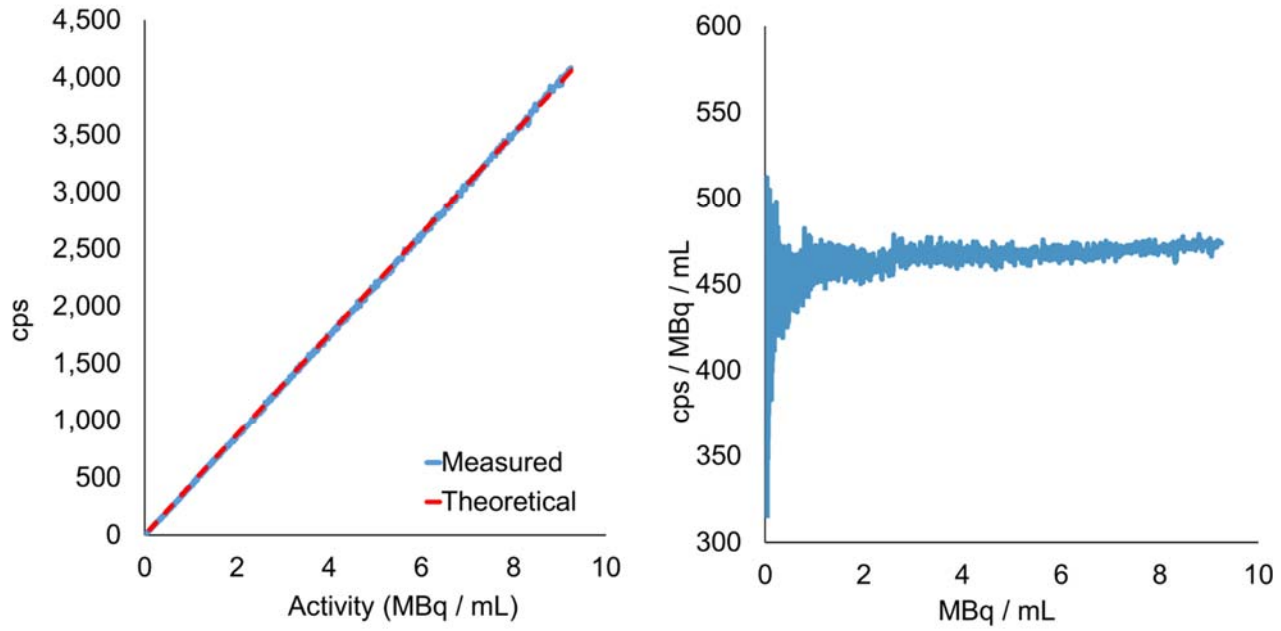


FIGURE 3. Detector linearity (A) and absolute sensitivity (B).

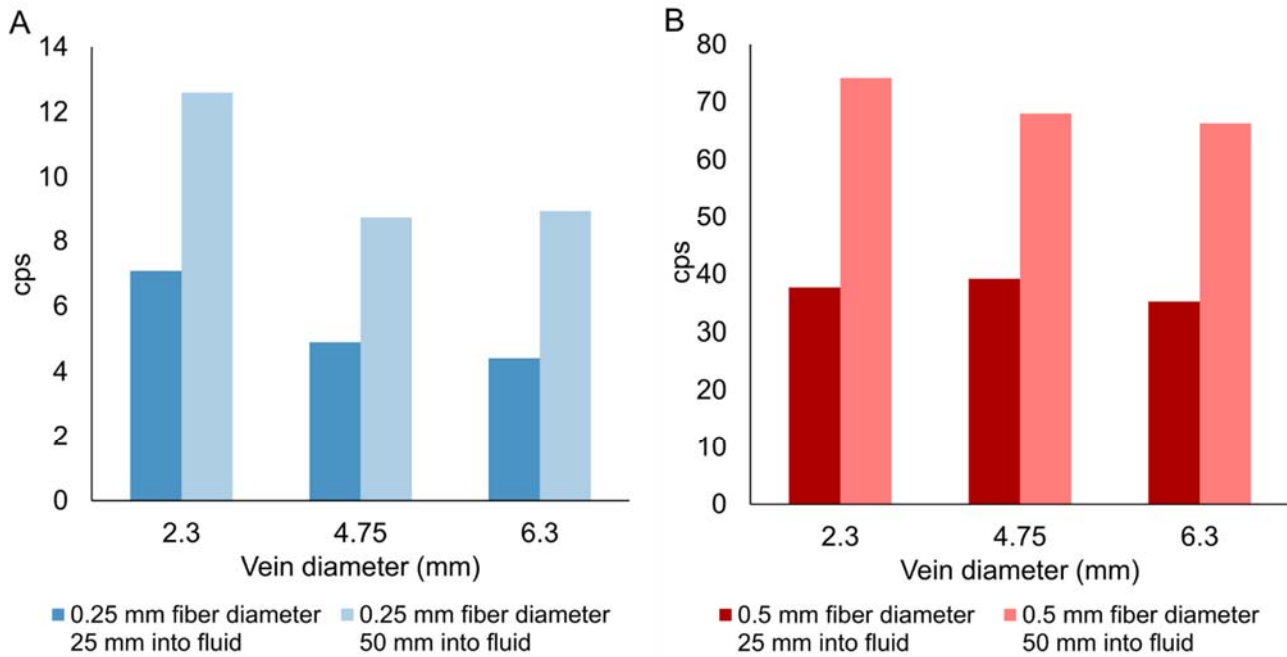


FIGURE 4. Background counts as a function of vein diameter at two different depths of insertion.

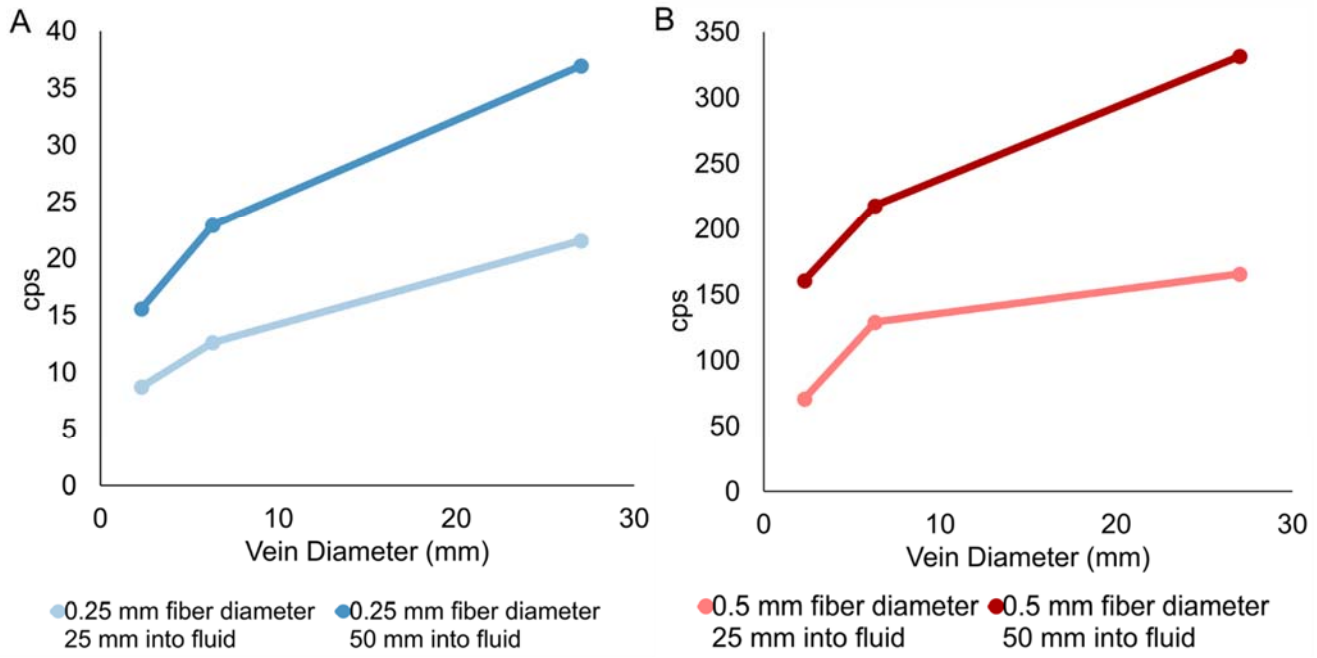


FIGURE 5. Impact of vein diameter.